Testing the Critical Window Hypothesis of Timing and Duration of Estradiol Treatment on Hypothalamic Gene Networks in Reproductively Mature and Aging Female Rats

Weiling Yin, Sean M. Maguire, Brian Pham, Alexandra N. Garcia, Nguyen-Vy Dang, Jingya Liang, Andrew Wolfe, Hans A. Hofmann, and Andrea C. Gore

Division of Pharmacology and Toxicology (W.Y., B.P., N.-V.D., J.L., A.C.G.), Departments of Integrative Biology (S.M.M., H.A.H.) and Psychology (A.N.G., A.C.G.), and Institute for Neuroscience (H.A.H., A.C.G.), The University of Texas at Austin, Austin, Texas 78712; and Johns Hopkins University School of Medicine (A.W.), Baltimore, Maryland 21287

At menopause, the dramatic loss of ovarian estradiol (E2) necessitates the adaptation of estrogen-sensitive neurons in the hypothalamus to an estrogen-depleted environment. We developed a rat model to test the "critical window" hypothesis of the effects of timing and duration of E2 treatment after deprivation on the hypothalamic neuronal gene network in the arcuate nucleus and the medial preoptic area. Rats at 2 ages (reproductively mature or aging) were ovariectomized and given E2 or vehicle replacement regimes of differing timing and duration. Using a 48-gene quantitative low-density PCR array and weighted gene coexpression network analysis, we identified gene modules differentially regulated by age, timing, and duration of E2 treatment. Of particular interest, E2 status differentially affected suites of genes in the hypothalamus involved in energy balance, circadian rhythms, and reproduction. In fact, E2 status was the dominant factor in determining gene modules and hormone levels; age, timing, and duration had more subtle effects. Our results highlight the plasticity of hypothalamic neuroendocrine systems during reproductive aging and its surprising ability to adapt to diverse E2 replacement regimes. (***Endocrinology*** **156: 0000–0000, 2015)**

The hypothalamic control of neuroendocrine function, energy balance, biological rhythms, and body temperature are highly sensitive to the estrogenic milieu (1–5). Thus, the profound depletion of ovarian estrogens with menopause in women requires the resetting of, and adaptation to, a new homeostatic environment. From animal studies, there is abundant evidence for cellular, physiological, and behavioral effects of estrogens (6–8) that likely underlie many of the neurobiological changes that occur during menopause in humans. Many of the most untoward menopausal symptoms, hot flashes, insomnia, weight gain, depression, and anxiety likely reflect maladaptive changes.

Until 2002, estrogens were widely used internationally to treat a variety of health-related symptoms caused by estrogen deficiency after surgical or natural menopause (9). That changed when results from the Women's Health Initiative seriously challenged the safety and utility of postmenopausal hormone treatment and was terminated early in 2002 (10), leading to a drastic reduction in prescriptions for postmenopausal symptoms. Since then, reanalysis of the Women's Health Initiative methods with regards to the age of participants, their choice of hormone treatment, and reference group suggested that there might exist a critical period at the perimenopause during which hormone treatment could benefit neurobiological and

ISSN Print 0013-7227 ISSN Online 1945-7170
Printed in USA

Received January 13, 2015. Accepted May 5, 2015.

Abbreviations: AG, aging; ARC, arcuate nucleus; BDNF, brain-derived neurotrophic factor; Cort, corticosterone; Ct, cycles threshold; E2, estradiol; ER, estrogen receptor; FDR, false discovery rate; HPA, hypothalamic-pituitary-adrenal; HPG, hypothalamic-pituitary-gonadal; HPT, hypothalamic-pituitary-thyroid; KNDy, kisspeptin-neurokinin B-prodynorphin; MAT, reproductively mature; mPOA, medial preoptic area; *Npy*, neuropeptide Y; OVX, ovariectomy; P4, progesterone; SCN, suprachiasmatic nucleus; WGCNA, weighted gene coexpression network analysis.

other health-related endpoints (11). Beyond this window, hormone treatments had no effect or were even detrimental (10). Despite increasing evidence for this critical window (12–16), "a definitive clinical trial to test this hypothesis is not feasible" (12) in humans due to clinical and ethical concerns. Therefore, developing and using an animal model to test this hypothesis toward discovery of underlying mechanisms is of major clinical and public health relevance. Our study focused on the hypothalamus, the brain region that drives the production of ovarian estrogens through the hypothalamic-pituitary-gonadal (HPG) axis, and is also sensitive to circulating estrogen feedback (17–19).

Here, we studied how chronological age, in conjunction with timing and duration of estradiol (E2) treatment relative to depletion, affected hypothalamic genes and neuroendocrine outcomes. We focused on 2 key hypothalamic regions, the arcuate nucleus (ARC) and the medial preoptic area (mPOA), which are major sites regulating energy balance, reproductive function, thermoregulation, and other homeostatic processes (20–23). Our goal was to provide mechanistic insights into gene networks involved in these functions, and their regulation by age, E2 deficiency, and E2 treatment, in a preclinical model of the menopause.

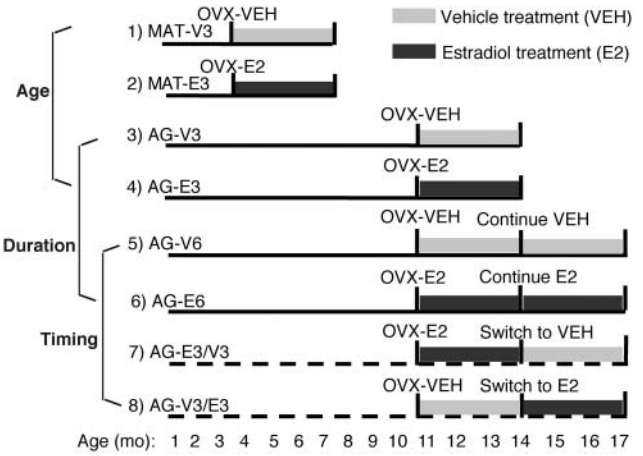

Figure 1. The experimental model used to study effects of age, timing, and duration of hormone treatment is shown. OVX surgery, and vehicle (VEH) or E2 capsule implantation were performed at age 4–5 and 11–12 months. Groups 1–6 included MAT and AG rats given VEH or E2 for 3 or 6 months. Groups 7 and 8 involved switching the hormone treatment given to AG rats 3 months after the OVX time point and allowing rats to age for another 3 months. Age effects were compared in groups 1–4 (2 variables, age and hormone). Duration of hormone effect was compared in groups 3–6 (2 variables, hormone and 3 or 6 months of duration). Effects of timing of hormone treatment were compared in groups 5–8.

Materials and Methods

Experimental animals, husbandry, and surgery

Female Sprague-Dawley rats were purchased at 3–4 months (reproductively mature [MAT] group; virgin) and 10–11 months old (reproductive aging [AG] group; retired breeder) from Harlan. Upon arrival, rats were randomly pair housed with a same-age partner in controlled room temperature (22°C) and light cycle (12-h light, 12-h dark cycle, lights on at 7 AM). Food and water were available ad libitum. The composition of the pelleted diet (PROLAB RMH 1800; PMI Nutrition Int'l, LLC) for rats is consistent through this research with crude protein (18% minimum), crude fat (5% minimum) and crude fiber (5% maximum). All of the animal experiments followed protocols approved by the Institutional Animal Care and Use Committee at the University of Texas at Austin and adhered to guidelines from The Guide for the Care and Use of Experimental Animals.

We used 8 groups of rats (n = 10 per group) (Figure 1). Rats were gently handled and general health checked twice a week upon arrival. After adapting to the new housing environment for a week, the estrous cycle of each rat was monitored for 2 weeks by performing daily vaginal lavage using sterile saline and recording cell morphology under an upright microscope at ×10 magnification. At age 3–4 months, rats with regular estrous cycles were used for the MAT group. At age10–11 months, rats with regular cycles (50%), irregular estrous cycles (30%), or persistent estrus (20%) were randomly assigned to different treatments for the AG groups (Figure 1). Bilateral ovariectomy (OVX) surgery was performed under isoflurane anesthesia as previously described, with rimadyl given for analgesia (24, 25). At the end of the surgery, a Silastic capsule was sc implanted intrascapularly. For both MAT and AG groups, capsules were prepared using 12.5-mm Corning Silastic tubing (1.98 mm inner diameter × 3.18 mm outer diameter) filled with either 5% 17β-estradiol (Sigma E-8875) in cholesterol (Sigma C-3292) for E2 treatment, or 100% cholesterol for vehicle treatment. Capsules were sealed with 1.5 mm Silastic glue (factor 2 medical grade) on each end, sterilized with chlorhexidine solution (2% chlorhexidine gluconate) and soaked in sterile normal saline overnight before surgery. Each cage was randomly assigned for the hormone treatment and rats within the same cage always received the same treatment. After OVX, all animals received a new identification number to allow blinded data collection. Body weight was monitored twice a week.

Tissue collection

Rats were humanely euthanized by decapitation after 3 or 6 months of hormone treatment, between 1 and 3 PM, 4–6 hours before lights off at 7 PM. A terminal trunk blood sample was collected and processed as described below. The brain was quickly extracted and briefly cooled in ice. Using an ice-cold brain matrix (Ted Pella, Inc) with coronal slots at 1 mm intervals to allow razor blade insertion, 8 coronal brain sections through the entire hypothalamus were collected. Each section was quickly immersed in 1.5 mL of RNAlater (Invitrogen, catalog AM7021M). After storage at 4°C overnight, each section was carefully mounted on a plain glass slide to be stored at −20°C.

At euthanasia, the pituitary was removed and weighed. The diameter of the uterine horn was measured at its base. The adrenal glands were carefully removed and weighed. The pituitary and adrenal index score were calculated by: [gland weight (mg)/body weight (g)] × 100.

RNA extraction and real-time PCR

RNAlater-treated brain sections were thawed once for the micropunching process. Hypothalamic regions containing the mPOA (bregma −0.26 to −1.80) and ARC (bregma −2.12 to −4.52) (26) were micropunched using a 1.2-mm diameter punch (Stoelting, 57399). RNA was extracted using RNAeasy Mini kit (QIAGEN, catalog 74104) according to the manufacturer's protocol. On-column deoxyribonuclease digestion was performed using RNase-Free DNase Set (QIAGEN, catalog 79254). RNA was eluted in 30-μL ribonuclease-free water and RNA quality and concentration were checked on the bioanalyzer using the Agilent RNA 6000 Nano kit (Agilent, catalog 5067–1511). A total of 200 ng of total RNA was converted to single-stranded cDNA using a high capacity cDNA reverse transcription kit (Applied Biosystems, catalog 4374966). Diluted cDNA samples (1 ng/μL for total 100 μL) were mixed with 100-μL TaqMan Universal PCR Master Mix (Applied Biosystems, catalog 4304437) and loaded on a customized 48-gene TaqMan Gene Expression Microfluidic Card (7900HT; Applied Biosystems). Genes related to energy balance, reproduction, circadian regulation, ovarian hormone signaling, and neurotransmitter signaling were specifically chosen and quantified in the mPOA and ARC. Real-time PCR was performed on an ABI ViiA7 machine as previously described (27). Relative expression of each gene was determined using the comparative cycles threshold (Ct) method (28–30). Each sample was normalized to 18s rRNA, which is constantly detected at 8 PCR Ct. All data were calibrated to the average change in Ct to the group mean of the AG-V6 group.

Serum hormone assays

After decapitation, trunk blood was collected and allowed to fully coagulate at room temperature. Serum was separated after centrifugation at 2300*g* for 5 minutes at room temperature and then stored at −80°C. Serum E2 concentration was measured in duplicates using an RIA kit (DSL-4800; Beckman Coulter) in one assay, with intraassay variability of 2.2%. Pituitary hormone concentrations were measured in 10-μL serum simultaneously in a single Milliplex Rat Pituitary Magnetic Bead assay (RPTMAG-86K; Millipore), with intraassay variability of LH 3.82%, FSH 2.25%, TSH 0.4%, ACTH 3.03%, GH 4.69%, prolactin 1.4%, and brain-derived neurotrophic factor (BDNF) 0.93%. To measure serum progesterone (P4), corticosterone (Cort), and thyroid hormones (total T_3 and T_4), 100 μL of serum were extracted using 150 μL of acetonitrile following the protocol of the Milliplex Steroid Magnetic Bead assay (STTHMAG-21K; Millipore), with intraassay variability of P4 4.93%, Cort 3.96%, T_3 10.94%, and T_4 7.63%. All magnetic bead assays were measured by the Luminex 200 system (Life Technologies) by Dr Andrew Wolfe (Johns Hopkins University School of Medicine).

Statistical analyses

Analysis of variance

All analysis was done using the statistical software package R (www.rproject.org). Many of our data were not normally distributed, therefore we used nonparametric permutation based ANOVA to compare group differences. Three sets of comparisons were made. 1) Effects of age were compared in groups 1–4 (Figure 1), in MAT and AG given vehicle or E2 for 3 months. This resulted in a 2-factor analysis, with variables age and hormone treatment. 2) Effects of duration were compared in groups 3–6 (Figure 1) in AG rats given vehicle or E2 for 3 or 6 months. This resulted in a 2-factor analysis, with variables hormone treatment and duration. 3) Effects of timing were tested using one-way ANOVA in groups 5–8 (Figure 1), with all animals used for a 6 month post-OVX period, but the treatments of E2 beginning either immediately or delayed by 3 months. Nonparametric post hoc Tukey contrasts were done with a multivariate Satterthwaite t-Approximation in the R package nparcomp. Statistical significance was considered at the 2-tailed $P < .05$.

Weighted gene coexpression network analysis (WGCNA)

WGCNA (31) is used to identify modules of highly correlated genes and representative module eigengenes (31). To generate weighted covariance networks of gene expression, a Pearson correlation matrix was calculated across all animals and treatment groups by computing pairwise correlations between all possible gene pairs. This was done separately for the 2 brain regions (mPOA and ARC). These correlation matrices were used to define networks where the connection strength between any pair of genes is given by the strength of their pairwise correlation. We subtracted each adjacency matrix from 1, creating a distance matrix of genes whose expression levels are highly correlated (low distance), or weakly correlated (high distance). Using this distance metric, we hierarchically clustered the genes and identified coexpression modules in the resulting dendrogram using a dynamic tree cutting algorithm available in the WGCNA R package, with a minimum module size of 5 genes. Expression values within each module were summarized using a statistic called an eigengene, which represents the first principal component of each module; this is the eigenvector of the covariance matrix that explains the largest amount of the variance. The eigengene summarizes the gene expression profile of the each set of correlated genes (each module) as a linear combination of the original gene expression values in the module that explains the most variance possible.

Body weight

We used the LME4 package in R to fit mixed-effect models with main effects of time, treatment group, and their interaction with a random effect that accounts for repeated measures of the same individuals. We then employed the lsmeans package in R to compute the least-squares means and compared Tukey contrasts for the treatment groups at each time point. *P* values from the mixed models are reported and results from the contrasts are summarized graphically using a compact letter display.

Covariance correlation analysis

We tested pairwise correlations between hypothalamic gene expression levels, serum hormone levels and physiological parameters (body weight, adrenal, and pituitary indices). To account for the effects of E2 treatment we included treatment (either E2 or vehicle) and the interaction between E2 treatment and each of the covariates listed above. The switch treatments (either E2 to vehicle or vehicle to E2) were assigned according to the final treatment they received at euthanasia. False discovery rate (FDR) correction (q value) was used to correct for multiple comparisons using the method of Benjamini and Hochberg (32).

Results

Hypothalamic gene expression was affected by age and E2 treatment

Brain regions from individuals in the 8 groups of rats (Figure 1) were used to identify modules of coregulated genes, analyzed by WGCNA. In the ARC, we identified 6 coexpression modules (Figure 2). In the mPOA, we identified 5 coexpression modules (Figure 3). A complete presentation of gene expression data is found in Supplemental Tables 1 and 2 for ARC and mPOA, respectively. Statistical results are summarized in Supplemental Table 3. In each brain region, we calculated representative eigengenes (the first principal component) for each module, which we used to analyze the effects of age (MAT vs AG), duration (3 mo vs 6 mo), and timing of hormone treatment (at OVX, or delayed by 3 mo) on gene expression.

In the ARC (Figure 2), 1 module (brown) was identified for which E2 treatment significantly down-regulated the representative eigengenes, irrespective of age, timing, or duration. A second module (blue) was identified for which the eigengenes were significantly up-regulated by E2, again independently of age, timing, or duration. Other modules had more complex responses to E2 status, with age, timing, and/or duration factoring into the results. The eigengene of the red module was significantly down-regulated by E2 ($P = .026$), and showed a trend for down-regulation with longer duration of treatment ($P = .058$). The turquoise module eigengene was significantly affected by age (MAT > AG), with a trend for an effect of E2 ($P = .065$). As a whole, ARC gene modules were substantially affected by E2 treatment and, to a lesser extent, age and E2 treatment duration. By contrast, the influence of timing of E2 treatment was relatively small; significant effects were identified in the brown and blue modules, driven by hormonal status (vehicle vs E2) at the time of tissue collection rather than timing of the onset of treatment (Supplemental Table 3).

In the mPOA (Figure 3), 5 clusters were identified, but there were fewer and less robust effects than in the ARC (Supplemental Table 3). E2 treatment significantly up-regulated the yellow module eigengene, and genes in this module were sensitive to E2 even when treatment was delayed for 3 months (Supplemental Table 3). The green module eigengene was significantly affected by age × E2 interaction ($P = .03$).

Serum hormones were sensitive to age and E2 treatment, timing, and duration

Twelve serum hormones were measured in the same experimental rats, with results shown in Figure 4 and statistics shown in Supplemental Table 3. Serum E2 concentrations were measured to confirm efficacy of our long-lasting Silastic capsules treatment (Figure 4A). In an earlier pilot study, we had measured E2 concentrations at 3 days, 1 month, 2 months, and 3 months OVX rats given E2 and found no significant differences of serum E2 among those groups, indicating that the hormone levels were maintained. E2 concentrations were significantly higher ($P = .001$) in mature compared with AG rats, although both fell into the physiological range as compared with samples collected from intact mature and AG rats for a different study (data not shown) but run in the same assay. In addition, in the reproductive AG group, serum E2 levels were not different between the AG-E3 and AG-E6 groups, again consistent with the constant release of hormone from the capsules. Serum LH and FSH were lowered by E2 (Figure 4, B and C), due to expected negative feedback effects. A significant difference between the AG-E6 and AG-V3/E3 ($P = .020$) was found for FSH, consistent with an effect of timing/duration of hormone treatment.

The hypothalamic-pituitary-thyroid (HPT) axis showed mixed effects of E2 treatment (Figure 4, D–F). Serum TSH and T_4 were significantly lowered by E2 treatment. Serum T_3 was significantly affected by duration of E2 treatment ($P = .023$) and duration × E2 interaction ($P = .013$). Rats with longer E2 treatment (6 mo) had lower serum T_3 compared with shorter E2 treatment (3 mo; AG-E3 vs AG-E6, $P = .0001$). Serum T_3 was also affected by age × E2 interaction ($P = .008$). AG E2-treated rats showed significantly elevated T_3 ($P = .032$), whereas MAT E2-treated rats showed a trend of lowered T_3 compared with vehicle rats. Comparing the AG 6-month-treated groups, E2 consistently lowered serum TSH ($P = .03$), T_3 ($P = .044$), and T_4 ($P < .001$); however, those hormones were differentially affected by the timing of E2 treatment (Supplemental Table 3).

The hypothalamic-pituitary-adrenal (HPA) axis was assessed through measures of serum ACTH (Figure 4G) and Cort (Figure 4H). ACTH was not affected in our model; however, the AG-V3 group showed large variability compared with all other groups (Figure 4G). For Cort, there was a significant age effect ($P = .031$) and an age × E2 interaction ($P = .028$). Serum P4, presumably from the adrenal in our OVX rats, was elevated by E2 (Figure 4I). Both age (age × E2 interaction, $P = .036$) and duration of E2 treatment ($P = .002$) affected serum P4 concentrations, and serum P4 was sensitive to E2 even when treatment was delayed for 3 months (Supplemental Table 3).

Serum PRL was significantly elevated by E2 treatment (Figure 4J). The pattern of serum GH after E2 treatment was complex (Figure 4K). A large variation was seen in the AG-V3 group, which showed a significant duration × E2

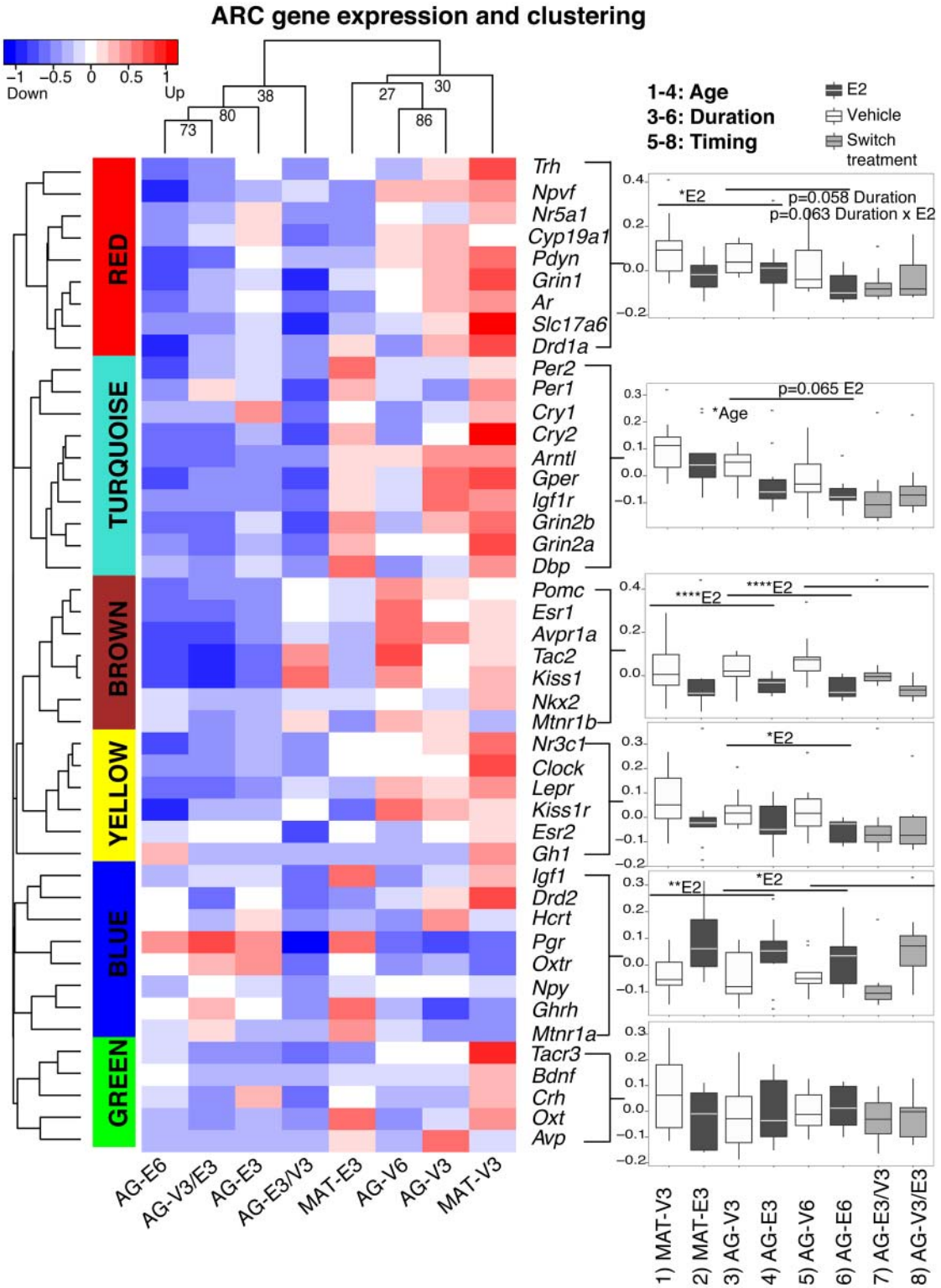

Figure 2. Modules of highly correlated genes in the ARC of the hypothalamus were identified by gene expression and clustering analysis. The hierarchical clustering dendrogram of 45 genes was cut to yield 6 color-coded modules. The gene expression heat map with blue-red representation was illustrated for each treatment group. Using a representative eigengene value, each module was plotted and analyzed to detect age, duration, and timing of hormone effects, and summarized in Supplemental Table 3. Significant *P* values are shown as *, $P < .05$; **, $P < .01$; ****, $P < .0001$. Trends ($0.05 < P < .1$) are also reported on the graphs. Treatment group correlations are shown on top of the heat map. Note that the ordering of groups on the heat map was determined by similarity of modules so the group orders are different from those shown in the box-and-whisker plots.

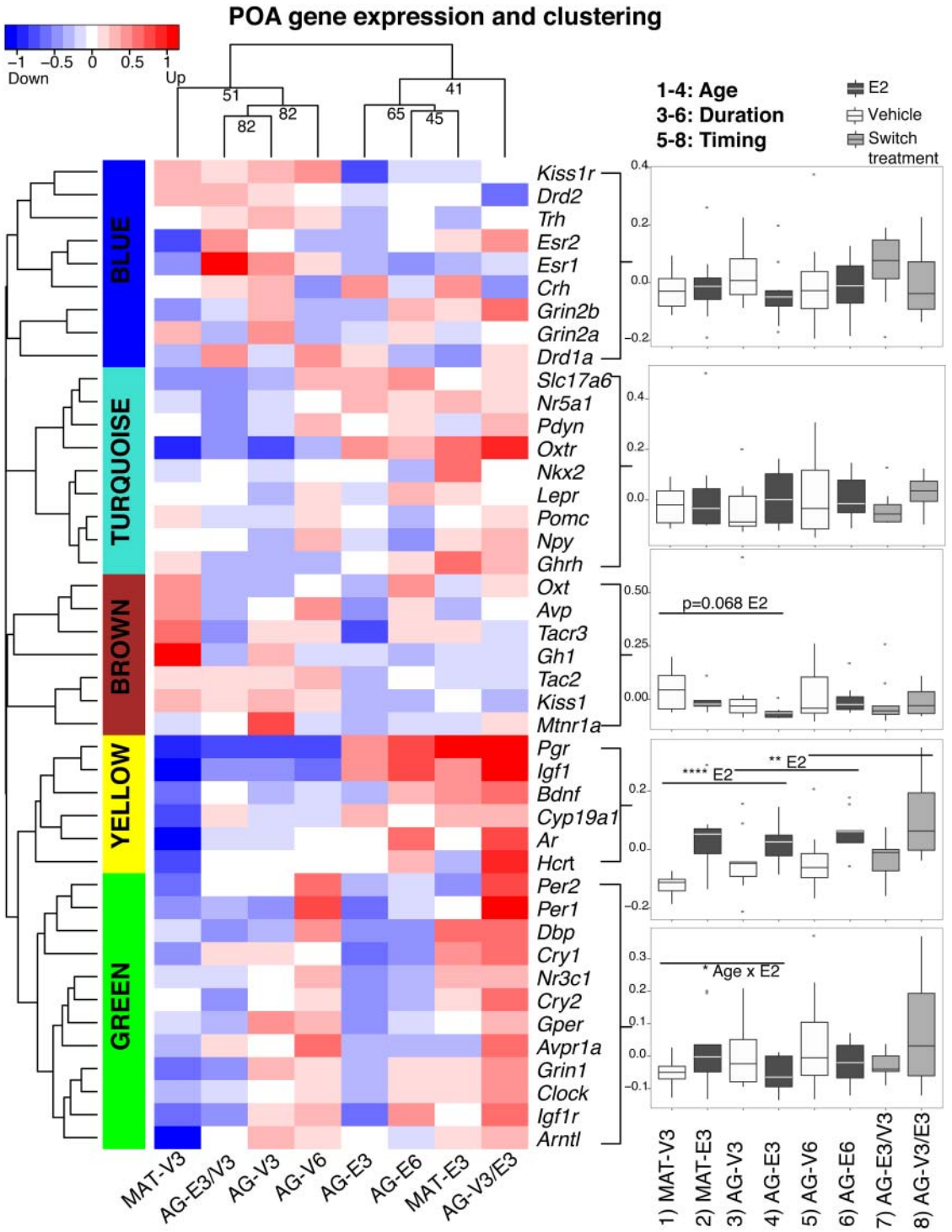

Figure 3. Modules of highly correlated genes in the mPOA were identified by gene expression and clustering analysis. A total of 43 genes were clustered into 5 color-coded modules. Data were analyzed and plotted as in Figure 2, and detailed statistics are shown in Supplemental Table 3.

interaction ($P = .0030$), a trend of duration ($P = .0593$), and an age × E2 interaction ($P = .074$). The AG-E6 group had significantly higher serum GH compared with AG-V6 ($P = .003$) (Supplemental Table 3). Finally, serum BDNF levels were significantly lower in E2 compared with vehicle-treated rats (Figure 4L).

Endocrine organs and body weight were sensitive to age, and timing and duration of E2 treatment

We assessed effects of E2 treatment on peripheral endocrine organs, namely, pituitary index, adrenal index, and uterine diameter. Data are shown in Supplemental Figure 1 and statistics in Supplemental Table 3. Compared

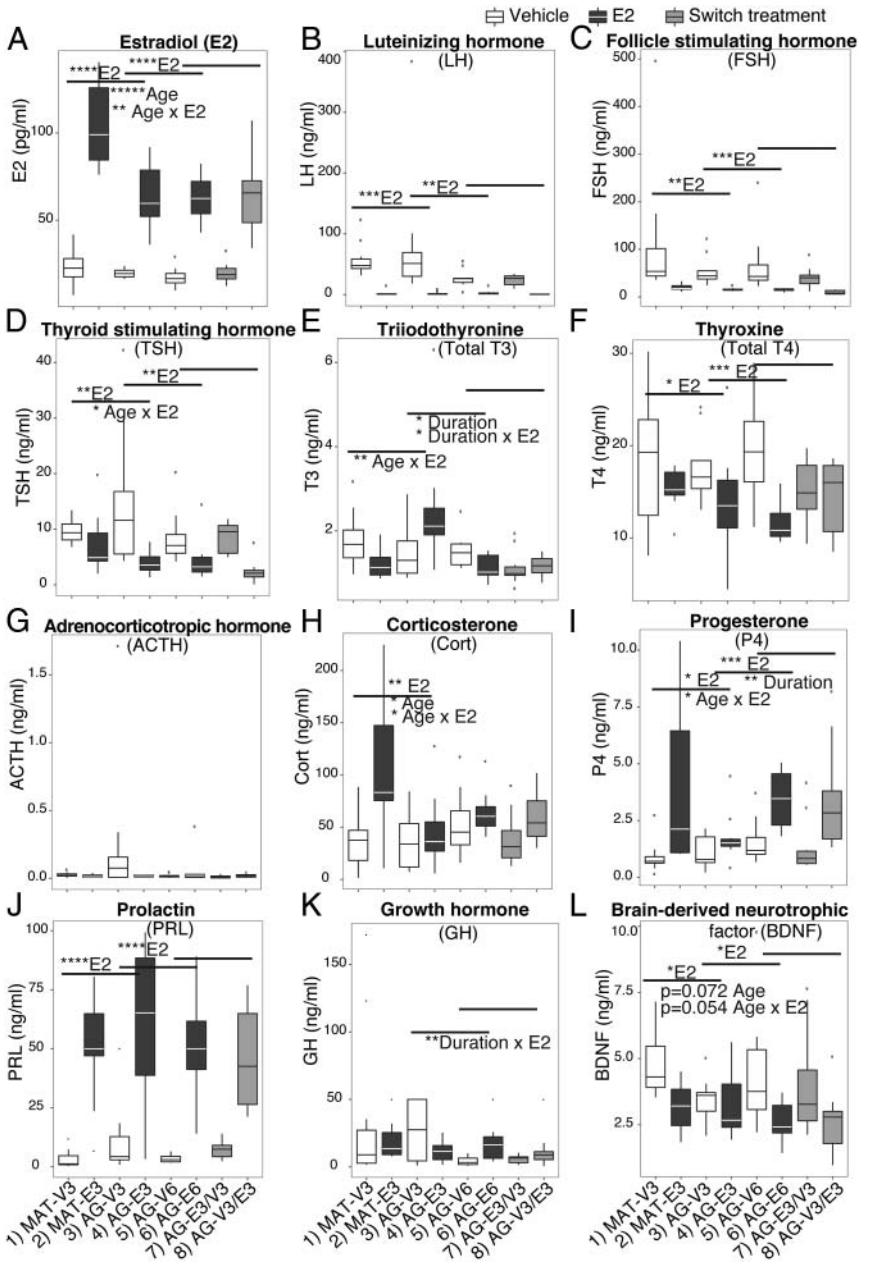

Figure 4. Serum concentrations of 12 hormones were differentially affected by age, and timing and duration of E2 treatment. Panels are organized for hormones involved in HPG axis (A–C), HPT axis (D–F), HPA axis (G–I), and growth and neurotropic factors (J–L). E2 treatment significantly elevated serum E2 (A), P4 (I), and PRL (J) and lowered LH (B), FSH (C), TSH (D), and T_4 (F). An age effect was shown for serum E2 (A), Cort (H), and BDNF (L). Age × E2 interaction effects were found for serum E2 (A), TSH (D), T_3 (E), Cort (H), P4 (I), and BDNF (L). A longer duration of E2 treatment significantly lowered T_3 (E) and elevated P4 (I). Significant *P* values are shown as *, $P < .05$; **, $P < .01$; ***, $P < .001$; ****, $P < .0001$. Trends ($0.05 < P < .1$) are also reported on the graph. n = 10 per group.

with vehicle counterparts, E2-treated rats showed higher pituitary and adrenal indices, and larger uterine diameter (Supplemental Figure 1). These endocrine organs were responsive to E2 treatment even when treatment was delayed for 3 months.

Body weight was extremely sensitive to E2 deficiency and treatment in our rat model. Beginning 10 days after OVX, body weight was significantly higher in E2-deficient rats compared with E2-treated rats in the MAT and AG groups over the 3 months after OVX period (Figure 5A). Notably, most of the body weight increase in vehicle rats occurred during the first month after OVX, after which body weight was relatively stabilized. In the 6 months AG groups (Figure 5B), switching the treatment after 3 months had profound effects on body weight, with most change happening in the first month postswitch.

Covariance analysis of hypothalamic gene expression, serum hormones, and physiological parameters

Significant correlations that survived FDR correction (q value) are shown in Figure 6 and listed in Supplemental Table 4. In the correlations between ARC gene expression module eigenvalues and hormones, we found several significant correlations (*P* value); however, none of the interaction effects were significant after FDR correction (q value) (Supplemental Table 4). In the correlation between mPOA module eigenvalues and hormones, only the significant correlations between serum P4 levels and the mPOA turquoise module (without interaction) survived FDR correction (q = 0.002) (Figure 6A). We used the same strategy to identify significant correlations between hormone levels and individual genes. As expected from the correlations between hormone levels and module eigengenes, serum P4 significantly correlated with *Oxtr*, *Lepr*, *Pomc*, *Ghrh*, and neuropeptide Y (*Npy*) from the mPOA, which all belonged to the mPOA turquoise module (Figure 6, B–F). We also found significant positive correlations between FSH levels and *Oxtr* (ARC), *Drd2* (ARC), and *Grin2a* (mPOA). Furthermore, serum Cort and *Ghrh* (mPOA) were significantly correlated (Figure 6G). In correlations between physiological parameters and hormone levels we found significant interaction ef-

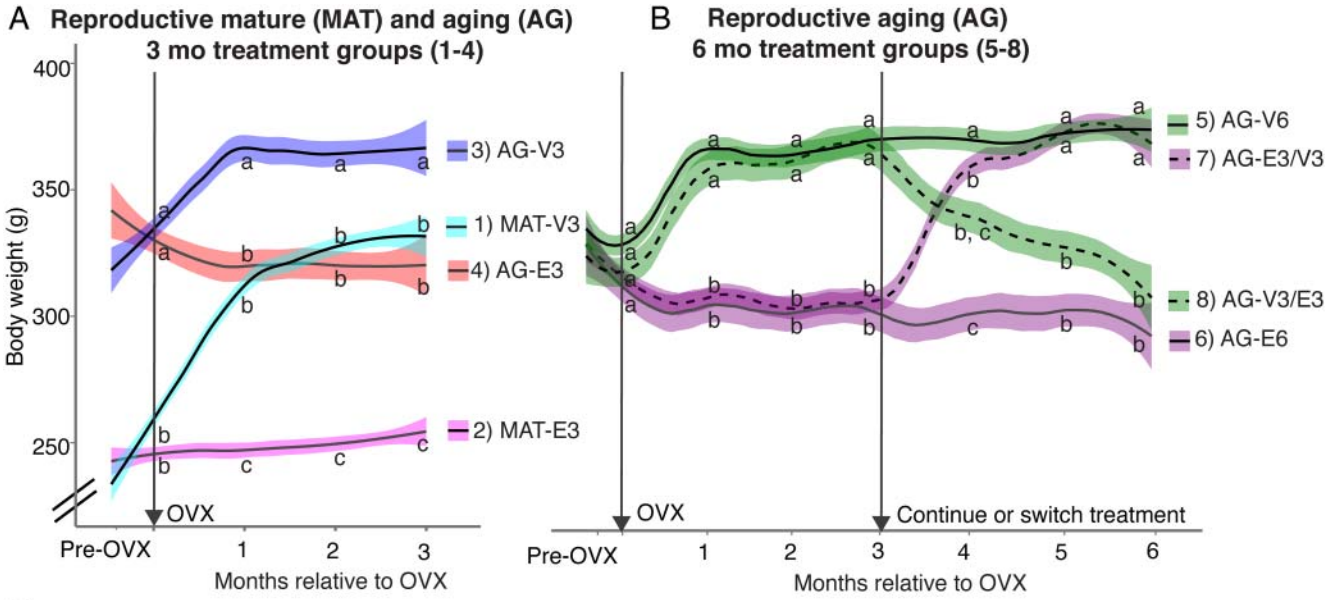

C **Repeated measures statistics within each group for changes over time**

Group ID	Months relative to OVX			
	Pre-OVX	1	2	3
1) MAT-V3	1	2	3	3
2) MAT-E3	1	1	1	1
3) AG-V3	1	2	2	2
4) AG-E3	2	1	1	1

Group ID	Months relative to OVX						
	Pre-OVX	1	2	3	4	5	6
5) AG-V6	1	2	2,3	3,4	3,4	4	4
6) AG-E6	2	1,2	1	1,2	1	1	1
7) AG-E3/V3	2	1,2	1	1	3	3,4	4
8) AG-V3/E3	1	3	3	4	2	1,2	1

Figure 5. Body weight was affected by age, and timing and duration of E2 treatment. A, In MAT and AG rats monitored for 3 months, body weight was significantly higher in vehicle-treated rats compared with E2-treated rats of both ages. B, Effects of 6 months of continuous vehicle or E2, or switching treatment at the 3-month time point, are shown for the AG rats. Body weight was sensitive to E2 status even after a 3-month delay in hormone treatment. n = 10 rats per group. Letters at each time point refer to groups that are similar (same letter) or significantly different (different letter). Group numbers correspond to numbering in Figure 1. C, Repeated measures ANOVA within each group identified body weight changes over the 3- to 6-month period, with numbers referring to levels being similar to (same number) or significantly different from (different number) other time points within that same group. Numbers 1–4 also represent body weight from lowest (1) to highest (4) within a group.

fects of GH and TSH with E2 treatment on pituitary index (Figure 6, H and I), such that each of these hormones correlated positively with pituitary index in the E2-treated group only. Serum E2 was positively correlated with adrenal index ($q < 0.0001$) (Figure 6J) and uterine diameter ($q = 0.035$) (Figure 6K) when tested without interaction effect. Serum P4 was marginally correlated with adrenal index ($P = .004$, $q = 0.057$). Physiological parameters showed strong correlations. Pituitary and adrenal indices were positively correlated when tested without interaction effect ($q = 0.026$) (Figure 6L). Adrenal index was negatively correlated with body weight at euthanasia ($q < 0.0001$) (Figure 6M).

Discussion

Our study systematically evaluated the effects of age, in conjunction with timing and duration of E2 treatment, on the dynamics of hypothalamic gene expression patterns in relation to physiological and hormonal responses. Overall, our results showed that E2 status was by far the dominant factor determining outcomes, with age, timing, and duration playing secondary roles. This result is of fundamental importance given the ongoing debates about E2 replacement therapy. Moreover, analysis of coexpression gene modules allowed us to gain detailed insights into groups of genes in 2 key hypothalamic regions that are correlated in their expression and responses to the experimental manipulations. Gene and hormone analyses also identified several significant effects of age, timing, and duration of hormone that may be relevant to the physiological effects of E2 on neuroendocrine functions.

Gene expression in the ARC is highly E2-responsive and includes kisspeptin-neurokinin B-prodynorphin (KNDy) neurons

We designed our PCR card to include genes in the hypothalamus involved in energy balance, circadian regulation, reproduction, neurotransmitter and hormone signaling. Our analysis identified several gene coexpression

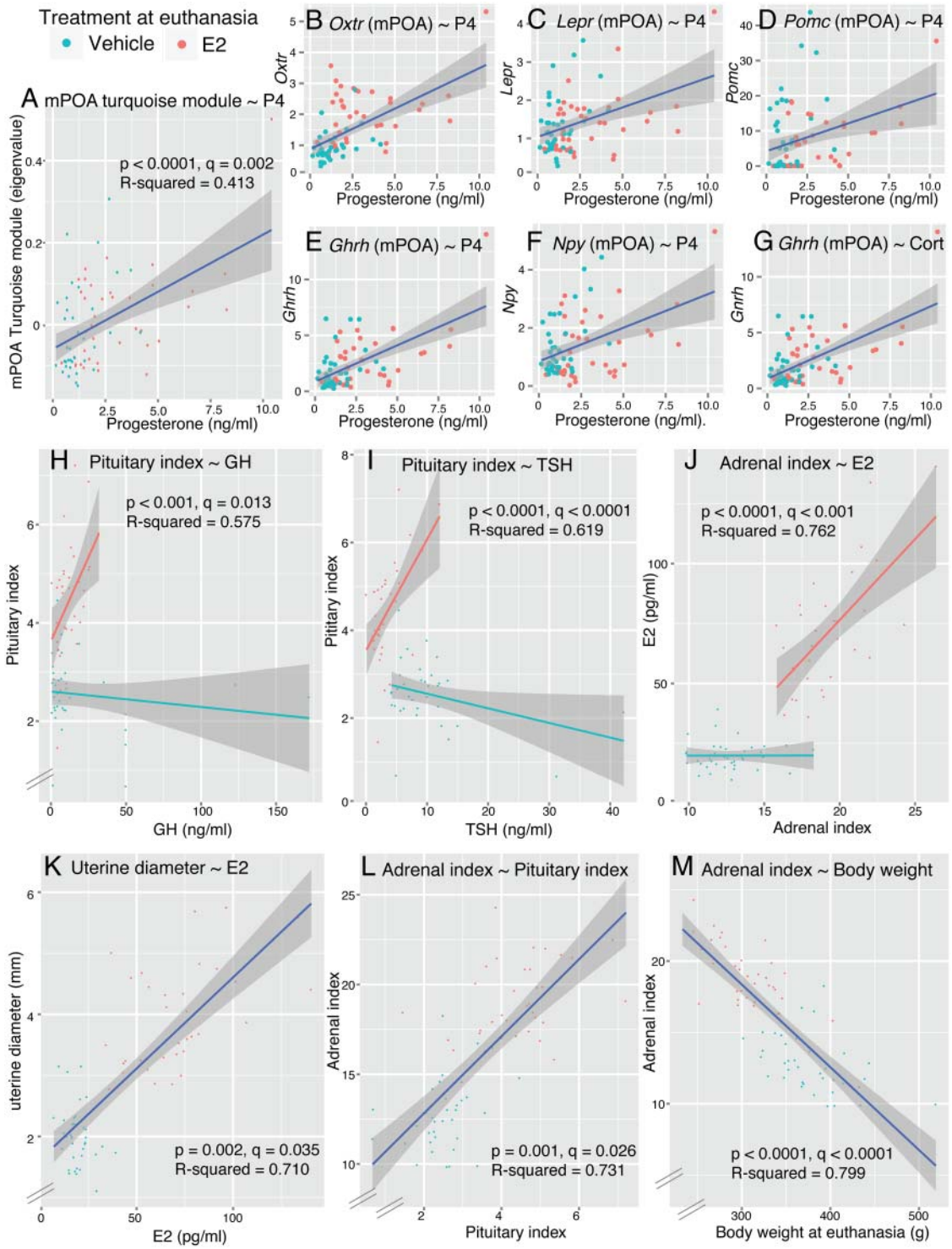

Figure 6. Correlations of hypothalamic gene expression, serum hormones, and physiological parameters. A, mPOA turquoise module eigenvalues positively correlated to serum P4. B–G, Significant correlations between individual mPOA gene expression and hormones are shown. Serum P4 correlated with *Oxtr*, *Lepr*, *Pomc*, *Ghrh*, and *Npy* (B–F), which all belonged to the mPOA turquoise module. G, Gene expression of *Ghrh* (mPOA) positively correlated with serum Cort. H–J, Correlations between physiological parameters and hormones. Correlations between pituitary index and GH (H), pituitary index and TSH (I), and adrenal index and E2 (J) were significant when tested with E2 and covariate interaction. Correlations between uterine diameter and E2 (K), adrenal index and pituitary index (L), and adrenal index and body weight (M) were significant when tested without E2 and covariates interaction. A statistical summary is provided in Supplemental Table 3.

modules for which E2 treatment was the dominant factor driving the clustering. Only 1 module (blue) was up-regulated by E2 treatment. Three modules showed down-regulation in response to E2 (red, brown, and yellow) with secondary effects of timing and trends for duration. The brown module was of particular interest as its genes were strongly down-regulated by E2 regardless of the timing and duration. This module comprised genes that include the estrogen receptor (ER)α (*Esr1*), KNDy signaling (*Kiss1* and *Tac2*), energy and electrolyte balance (*Pomc* and *Avpr1a*), melatonin responsiveness (*Mtnr1b*), and neuronal differentiation (*Nkx2.1*).

KNDy neurons in the ARC coexpress *Esr1* (33–37) and are a central node in the control of GnRH secretion (38–44). KNDy neurons are sexually dimorphic (37, 45, 46), hormone-responsive (47, 48), and are critically involved both in reproductive function and energy balance (40–44, 49). As shown previously, the population of KNDy neurons in the ARC exhibits E2- and age-related morphological changes such as neuronal hypertrophy and cell loss (35, 50–54). It is established that hypothalamic *Kiss1* and *Tac2* are elevated in parallel with diminished serum E2 and increased GnRH/LH release in postmenopausal women, macaques (47, 51, 55), and OVX rodents (33, 42, 56). Our gene coexpression analysis provides a unique way to examine the KNDy pathway in a manner that provides insights to several important neuroendocrine systems. Consistent with previous reports (33, 47, 51, 55, 56), expression of kisspeptin (*Kiss1*) and neurokinin-B (*Tac2*) in our rats' ARC brown module was strongly down-regulated by E2 treatment. In the red module, prodynorphin (*Pdyn*) was down-regulated by E2 with a trend in the duration analysis. This agrees with other studies showing differences in the gene expression pattern between *Pdyn* with *Kiss1* and *Tac2* (40) and adds in the age and duration analysis. The differential clustering of *Pdyn* and *Kiss1/Tac2* might also be related to changes of non-KNDy prodynorphin neurons and neurokinin-B neurons in the ARC. The receptor targets of KNDy neurons have mainly been studied on the regulation of GnRH neurons and reproductive function (39–44). In our study, gene expression of kisspeptin receptor (*Kiss1r*) in the yellow module was not as robustly down-regulated by E2 as its corresponding ligand, *Kiss1*, in the brown module. The neurokinin B receptor (*Tacr3*) was in the green module, which was the only module not affected by age and/or E2 in the ARC. Our data agree with the suggestion that the modulation of KNDy ligand-receptor pathways in the ARC (and median eminence) is mediated primarily through ligand synthesis rather than receptor modulation (47). Furthermore, these data show differential effects of age and duration of E2 but no effects of timing.

Energy balance genes in the ARC

Beyond the KNDy neurons were other energy balance genes in the ARC, including proopiomelanocortin neurons (*Pomc*), *Npy*, orexin (*Hcrt*), and *Ghrh*, all of which were strongly regulated by E2 status. *Pomc* was clustered in the brown module, together with *Kiss1*, *Tac2*, and *Esr1*, and strongly down-regulated by E2. *Npy*, *Hcrt*, and *Ghrh* were clustered in the blue module, the only module up-regulated by E2 treatment.

Circadian genes in the ARC

Although the central circadian clock is located in the suprachiasmatic nucleus (SCN) of the hypothalamus (57–60), it communicates with other hypothalamic and extra-hypothalamic regions, each of which contains intrinsic clock gene expression. We found a correlated cluster in the ARC (turquoise) that was down-regulated by age and, to a lesser extent E2, that included the circadian genes *Per1*, *Per2*, *Cry1*, *Cry2*, *Dbp*, and *Arntl* (61–65). The function of circadian related genes and estrogen signaling are tightly interlinked; *Clock* mutant mice demonstrate disrupted estrous cycles (66, 67), and fluctuations of steroid hormone secretion through the estrous cycle affect *Clock* expression in the SCN (68, 69). The role of circadian genes in other hypothalamic nuclei is not well established (70), but there is evidence that *Per1* expression in ARC neurons exhibits a diurnal rhythm paralleling that of the SCN (71). Our finding of age-related decreases in gene expression of this cluster is consistent with evidence for age-associated changes of circadian gene expression and protein synthesis in the SCN (70, 72). Future studies of the function of the circadian genes in ARC should include analyses across multiple time points around the 24-hour clock, to better understand the impact of estrogen and aging on chronobiological systems (73–75).

The mPOA gene network was modestly affected by E2 and aging

E2 had significant effects on one module in the mPOA (yellow), with expression increased in all groups by E2 status at euthanasia. The yellow gene module contains genes involved in hormone signaling and synthesis (*Pgr*, androgen receptor [*Ar*], and *Cyp19a1*), neurotropic factors (*Igf1* and *Bdnf*), and Orexin (*Hcrt*), which play important roles in sleep (76) and feeding behavior (77). Three of these same genes were also up-regulated by E2 in the ARC (blue module): *Igf1*, *Hcrt*, and *Pgr*. In the mPOA, *Cyp19a1* (the aromatase p450 gene) and *Ar* were up-regulated by E2 but were down-regulated by E2 treatment in the ARC, indicative of region-specific differences in androgen metabolism and signaling. The *Kiss1/Tac2* expression in the mPOA was not robustly affected as in the ARC,

with only a trend of down-regulation (brown module, $P = .068$) in E2-treated compared with E2-deficient rats. Kisspeptin neurons in the POA (specifically the anteroventral periventricular nucleus) are suggested to be a target of estrogen positive feedback and regulated positively by E2 (33, 78). Our results suggest possible functional changes of kisspeptin neurons in response to long-term OVX and E2 treatment. Other differences between gene expression in the mPOA and ARC are not surprising given the functional differences played by these nuclei, their differential inputs and outputs, differences in neuronal phenotypes within each region (20–23), and differential involvement of these regions in the mediation of positive and negative feedback effects of E2 (79–82).

Many circadian genes in the mPOA were clustered together, including the same 6 that clustered in the ARC (*Per1*, *Per2*, *Dbp*, *Cry1*, *Cry2*, and *Arntl*), along with *Clock*. However, the pattern of expression of these circadian genes differed between the 2 regions (decreased by age in the ARC; age by E2 interaction in the mPOA). Similar to our ARC results, these circadian genes in the mPOA also clustered with *Igf1r*, *Grin1*, and *Gper*. These correlated modules identified by WGCNA analysis have enabled us to identify novel gene relationships and establish directions for future study.

Serum hormone responses were more sensitive to the timing and duration of E2

The hypothalamic-anterior pituitary neuroendocrine systems are well known to undergo age-related changes and to be modulated by E2 (83, 84), presumably via the expression of ERs in hypothalamic nuclei such as the ARC and mPOA (8, 85, 86). Furthermore, 90% of anterior pituitary cells contain nuclear ERα (87). As expected, pituitary indices were higher in E2 than vehicle rats, consistent with the known pituitary hypertrophy caused by E2 treatment (88), and uterine diameter was also higher due to the uterotrophic actions of E2 (89). Adrenal index was also robustly increased in all groups with E2 on board at the time of euthanasia.

To gain insights into the question of age, and timing and duration of E2 treatment, we measured levels of the anterior pituitary hormones and target hormones and further analyzed their correlations with hypothalamic gene expression. The serum gonadotropins LH and FSH were strongly suppressed by E2 treatment regardless of the timing and duration, consistent with earlier studies showing this negative feedback (90).

The HPT axis is a target for E2 action (91–94), and the close interaction between the HPG and the HPT pathways may relate to the increased and often undiagnosed frequency of thyroid disorders in menopausal women (95, 96). However, the literature concerning estrogenic effects on the thyroid system is inconsistent, with increases, decreases, or no change reported in various models, and dependent upon which thyroid hormone(s) are measured and duration of treatment (91–94, 96–98). Due to the limitation of the assay, we only studied the serum TSH, total T_3, and total T_4. Our model revealed complex effects of E2 and age on the HPT system. Serum TSH and total T_4 were significantly lower in E2 rats compared with vehicle-treated rats. However, delayed E2 treatment down-regulated TSH, but not T_4, suggesting a disassociation of the HPT axis in response to delayed E2 treatment. Total T_3 was differentially regulated by E2 dependent upon age, duration, and timing. The differential response of T_3 and T_4 towards E2 treatment suggests the possibility of changes in hormone synthesis in the thyroid gland. Enzyme activity involved in thyroid hormone synthesis, conversion, and transportation might be altered with age and E2 status. Clearly more research is needed to resolve these discrepancies and to gain more insight as to the differential responses of the thyroid axis hormones to E2.

HPA measures showed no difference in ACTH, and elevated Cort in the MAT E2 rats. E2 enhances HPA responses to stress in OVX rats (99–101), but we did not administer any stressor so we do not know why only the MAT rats responded to E2 with higher Cort concentrations. It should be noted that our replacement levels of E2 were somewhat higher in the MAT compared with AG rats; therefore a dose effect should be considered in interpreting these data. The elevation in serum P4 in our E2-treated groups, presumably from adrenal and possibly adipose tissue (102), was surprising. Despite evidence that E2 treatment elevates P4 receptor in the hypothalamus (103) and pituitary (104), we could not locate any literature linking E2 to peripheral P4 synthesis in an OVX model. Moreover, serum P4 positively correlated with gene expression of *Ghrh*, *Npy*, *Pomc*, *Lepr*, and *Oxtr* in the mPOA. In the literature on OVX rats, endogenous serum P4 is nearly always ignored, and the mechanism behind our finding needs further study.

Serum prolactin was significantly elevated in E2-treated rats independent of age, duration, and timing of treatment, consistent with the literature (105, 106). There was a highly significant duration by E2 interaction on GH levels. Finally, we analyzed serum BDNF whose circulating levels were significantly decreased by E2 treatment, even though neural *Bdnf* gene expression was up-regulated by E2 treatment in the mPOA (yellow module) and unaffected in the ARC (green module). Hypothalamic BDNF is an important regulator of energy balance and feeding behavior (107). Interactions between E2 and the BDNF signaling pathway have been reported in the central

nervous system (108) but not in the periphery. The source of peripheral BDNF production is still unclear (109, 110); however, the anterior pituitary lobe (109) and platelets (111) store and release BDNF. Our data provide more insights to how age and timing of E2 treatment could possibly play differential roles in the central and peripheral BDNF system.

Body weight was remarkably sensitive to E2 deficiency and treatment, even if timing of treatment was delayed

Many menopausal women undergo weight gain and accumulation of visceral fat (7, 112, 113). Significant weight gain is linked to postmenopausal morbidity such as cardiovascular disease and metabolic syndrome (114). A rapid weight gain phenotype is well established in E2-deficient animal models (115–119). Consistent with this, our E2-deficient OVX rats gained body weight, whereas E2-treated rats maintained their body weight similar to ovarian intact rats (the latter data were monitored as part of a separate ongoing study on AG intact rats). Our model also uniquely demonstrated the sensitivity of body weight change relevant to the timing and duration of E2 treatment. Here, we showed a totally reversed body weight pattern after switching treatment (E2 to vehicle or vehicle to E2) indicating a remarkable E2-dependent metabolic regulation. In testing the "critical window" hypothesis, we found that early E2 treatment showed no benefit in maintaining body weight 6 months after OVX if treatment was terminated 3 months post-OVX.

In the 6-month continuous vehicle treatment groups (no switch), body weight reached a plateau in 1–2 months. Consistent with this, the ARC blue and brown gene modules containing most of the energy balance genes showed similar expression at the 3- and 6-month points. These 2 modules showed a totally reversed pattern after switching treatment, which was also consistent with a totally reversed pattern of body weight. It has already been reported that food intake increases only transiently after OVX in rodent models (120, 121), and pilot data in our lab measuring food consumption in OVX rats showed that any changes to food intake normalized after about 2 months (data collected in a different cohort, not shown here). Based on the effects of E2 on body weight, one would expect an inhibition of the NPY pathway (orexigenic, increase appetite) and an elevation of the POMC pathway (anorexic, decrease appetite) after E2 treatment. However, we showed a prolonged gene expression elevation (*Npy*, *Hcrt*, and *Ghrh*) and suppression (*Pomc*, *Kiss1*, and *Tac2*) by E2 compared with vehicle treatment. Our somewhat opposite results might reflect compensatory changes of energy balance neurons in the ARC after a major primary action of E2 affecting energy expenditure. Presumably, changes of energy expenditure, not energy intake is essential to maintain this body weight differential (7) as has been seen in OVX rats (122), aromatase-deficient mice (117), and ERα knockout mice (116). Those genes might be involved in the maintenance of a new homeostatic setpoint, which over time is not reflected by food intake. Taken together, our results indicate a remarkable sensitivity and plasticity of the central network of energy balance neurons in response to E2 and other peripheral signals.

Limitations and clinical implications

Although the OVX rodent is a well-established model for hormone deprivation at menopause (25, 43, 123, 124), there are several caveats. Only humans and nonhuman primates undergo a true menopause, and there are species differences even among primates (125). Several rodent models exist beyond OVX, including the 4-vinylcyclohexene-diepoxide model of ovotoxicity that results in premature follicular loss (126–129). We believe that several features of our rat model add substantially to this study's clinical relevance. First, we used rats at ages that enabled a dissociation of the effect of chronological age comparable to pre- and perimenopausal women. In fact, although the dominant influence on the gene networks was E2 treatment, age played a significant role in several outcomes. Second, the shorter lifespan of rats enabled us to systematically test immediate vs delayed E2 treatment and for different durations. Third, rodent models enable direct links to be drawn between hypothalamic neuronal properties and neuroendocrine outcomes, something not feasible in humans and not practical in nonhuman primates. Thus, this systematic analysis of effects of E2 has shed light on neurobiological responsiveness and identified potential hypothalamic targets that can be further explored for functional outcomes and underlying molecular mechanisms.

Conclusions

This study provided a tool to examine the critical window hypothesis. Our results showed novel insights into how the timing and duration of E2 treatment and chronological age interact to affect expression of genes in the ARC and mPOA involved in neuroendocrine function. These results underscore the point that the presence/absence of E2 replacement at the time of gene expression measurements dominated the outcomes. Although fewer endpoints were sensitive to age, timing, and/or duration, those that we identified will point the way to understanding the biological relevance. Although gene clusters were identified in

ARC and mPOA, there were substantial regional differences in how they responded to age and/or E2, with the ARC overall much more responsive to the hormone treatments than the mPOA. In the ARC, E2 differentially affected clusters of genes included KNDy, energy balance, and circadian genes. In the mPOA, the most affected gene cluster was up-regulated by E2. Our hormone data also suggest some disconnection between the central and peripheral endocrine systems. As suggested by the HPA and HPT axis results, the timing and duration of E2 treatment differentially affected pituitary and peripheral endocrine organ functions. Overall, our data underscore the sensitivity and plasticity of the neuroendocrine system in response to E2 status.

Acknowledgments

We thank Dr Deena M. Walker and Dr Bailey A. Kermath for optimizing the gene expression assays in the Gore laboratory. We also thank our wonderful undergraduates Xutong Wang, Haben Tesfamariam, Kelsey Bezner, Ji Eun Kim, Christina Depena, and Atlantys E. Carroll for assisting with animal work and tissue collection.

Address all correspondence and requests for reprints to: Andrea C. Gore, PhD, Division of Pharmacology and Toxicology, The University of Texas at Austin, 107 West Dean Keeton, C0875, Austin, TX 78712. E-mail: andrea.gore@austin.utexas.edu.

This work was supported the National Institutes of Health Grant AG16765 and Baltimore Diabetes Research Center Integrated Physiology Core Grant P60 DK079637.

Disclosure Summary: The authors have nothing to disclose.

References

1. **Frank A, Brown LM, Clegg DJ.** The role of hypothalamic estrogen receptors in metabolic regulation. *Front Neuroendocrinol*. 2014; 35:550–557.
2. **Cusmano DM, Hadjimarkou MM, Mong JA.** Gonadal steroid modulation of sleep and wakefulness in male and female rats is sexually differentiated and neonatally organized by steroid exposure. *Endocrinology*. 2014;155:204–214.
3. **Israel DD, Sheffer-Babila S, de Luca C, et al.** Effects of leptin and melanocortin signaling interactions on pubertal development and reproduction. *Endocrinology*. 2012;153:2408–2419.
4. **Musatov S, Chen W, Pfaff DW, et al.** Silencing of estrogen receptor α in the ventromedial nucleus of hypothalamus leads to metabolic syndrome. *Proc Natl Acad Sci USA*. 2007;104:2501–2506.
5. **Qiu J, Bosch MA, Tobias SC, et al.** A G-protein-coupled estrogen receptor is involved in hypothalamic control of energy homeostasis. *J Neurosci*. 2006;26:5649–5655.
6. **Rao YS, Mott NN, Wang Y, Chung WC, Pak TR.** MicroRNAs in the aging female brain: a putative mechanism for age-specific estrogen effects. *Endocrinology*. 2013;154:2795–2806.
7. **Mauvais-Jarvis F, Clegg DJ, Hevener AL.** The role of estrogens in control of energy balance and glucose homeostasis. *Endocr Rev*. 2013;34:309–338.
8. **Chakraborty TR, Hof PR, Ng L, Gore AC.** Stereologic analysis of estrogen receptor α (ER α) expression in rat hypothalamus and its regulation by aging and estrogen. *J Comp Neurol*. 2003;466:409–421.
9. **Hersh AL, Stefanick ML, Stafford RS.** National use of postmenopausal hormone therapy: annual trends and response to recent evidence. *JAMA*. 2004;291:47–53.
10. **Rossouw JE, Anderson GL, Prentice RL, et al.** Risks and benefits of estrogen plus progestin in healthy postmenopausal women: principal results From the Women's Health Initiative randomized controlled trial. *JAMA*. 2002;288:321–333.
11. **Santen RJ, Allred DC, Ardoin SP, et al.** Postmenopausal hormone therapy: an Endocrine Society scientific statement. *J Clin Endocrinol Metab*. 2010;95:s1–s66.
12. **Maki PM.** Critical window hypothesis of hormone therapy and cognition: a scientific update on clinical studies. *Menopause*. 2013; 20:695–709.
13. **Daniel JM.** Estrogens, estrogen receptors, and female cognitive aging: the impact of timing. *Horm Behav*. 2013;63:231–237.
14. **Whitmer RA, Quesenberry CP, Zhou J, Yaffe K.** Timing of hormone therapy and dementia: the critical window theory revisited. *Ann Neurol*. 2011;69:163–169.
15. **Hamilton RT, Rettberg JR, Mao Z, et al.** Hippocampal responsiveness to 17β-estradiol and equol after long-term ovariectomy: implication for a therapeutic window of opportunity. *Brain Res*. 2011;1379:11–22.
16. **Maki PM, Dennerstein L, Clark M, et al.** Perimenopausal use of hormone therapy is associated with enhanced memory and hippocampal function later in life. *Brain Res*. 2011;1379:232–243.
17. **Caligaris L, Astrada JJ, Taleisnik S.** Release of luteinizing hormone induced by estrogen injection into ovariectomized rats. *Endocrinology*. 1971;88:810–815.
18. **Bronson FH, Vom Saal FS.** Control of the preovulatory release of luteinizing hormone by steroids in the mouse. *Endocrinology*. 1979;104:1247–1255.
19. **Gore AC.** GnRH pulsatility. In: *GnRH: The Master Molecule of Reproduction*. Boston, MA: Kluwer, 2002:29–52.
20. **Cowley MA, Smart JL, Rubinstein M, et al.** Leptin activates anorexigenic POMC neurons through a neural network in the arcuate nucleus. *Nature*. 2001;411:480–484.
21. **Shimada M, Tritos NA, Lowell BB, Flier JS, Maratos-Flier E.** Mice lacking melanin-concentrating hormone are hypophagic and lean. *Nature*. 1998;396:670–674.
22. **Nagel JA, Satinoff E.** Mild cold exposure increases survival in rats with medial preoptic lesions. *Science*. 1980;208:301–303.
23. **Powers B, Valenstein ES.** Sexual receptivity: facilitation by medial preoptic lesions in female rats. *Science*. 1972;175:1003–1005.
24. **Yin W, Mendenhall JM, Bratton SB, et al.** Novel localization of NMDA receptors within neuroendocrine gonadotropin-releasing hormone terminals. *Exp Biol Med*. 2007;232:662–673.
25. **Yin W, Wu D, Noel ML, Gore AC.** Gonadotropin-releasing hormone neuroterminals and their microenvironment in the median eminence: effects of aging and estradiol treatment. *Endocrinology*. 2009;150:5498–5508.
26. **Paxinos GWC.** *The Rat Brain in Stereotaxic Coordinates*. San Diego, CA: Academic Press, 1986:18–34.
27. **Walker DM, Juenger TE, Gore AC.** Developmental profiles of neuroendocrine gene expression in the preoptic area of male rats. *Endocrinology*. 2009;150:2308–2316.
28. **Livak KJ, Schmittgen TD.** Analysis of relative gene expression data using real-time quantitative PCR and the $2(-\Delta\Delta C(T))$ method. *Methods*. 2001;25:402–408.
29. **Pfaffl MW.** A new mathematical model for relative quantification in real-time RT-PCR. *Nucl Acids Res*. 2001;29:e45.

30. **Schmittgen TD, Livak KJ.** Analyzing real-time PCR data by the comparative C(T) method. *Nat Protoc*. 2008;3:1101–1108.
31. **Langfelder P, Horvath S.** WGCNA: an R package for weighted correlation network analysis. *BMC Bioinformatics*. 2008;9:559.
32. **Benjamini Y, Hochberg Y.** Controlling the false discovery rate: a practical and powerful approach to multiple testing. *J Royal Stat Soc Series B*. 1995;57:289–300.
33. **Smith JT, Cunningham MJ, Rissman EF, Clifton DK, Steiner RA.** Regulation of Kiss1 gene expression in the brain of the female mouse. *Endocrinology*. 2005;146:3686–3692.
34. **Burke MC, Letts PA, Krajewski SJ, Rance NE.** Coexpression of dynorphin and neurokinin B immunoreactivity in the rat hypothalamus: morphologic evidence of interrelated function within the arcuate nucleus. *J Comp Neurol*. 2006;498:712–726.
35. **Rance NE, Young WS 3rd.** Hypertrophy and increased gene expression of neurons containing neurokinin-B and substance-P messenger ribonucleic acids in the hypothalami of postmenopausal women. *Endocrinology*. 1991;128:2239–2247.
36. **Goodman RL, Lehman MN, Smith JT, et al.** Kisspeptin neurons in the arcuate nucleus of the ewe express both dynorphin A and neurokinin B. *Endocrinology*. 2007;148:5752–5760.
37. **Goubillon ML, Forsdike RA, Robinson JE, Ciofi P, Caraty A, Herbison AE.** Identification of neurokinin B-expressing neurons as an highly estrogen-receptive, sexually dimorphic cell group in the ovine arcuate nucleus. *Endocrinology*. 2000;141:4218–4225.
38. **Lehman MN, Coolen LM, Goodman RL.** Minireview: kisspeptin/neurokinin B/dynorphin (KNDy) cells of the arcuate nucleus: a central node in the control of gonadotropin-releasing hormone secretion. *Endocrinology*. 2010;151:3479–3489.
39. **Ohkura S, Takase K, Matsuyama S, et al.** Gonadotrophin-releasing hormone pulse generator activity in the hypothalamus of the goat. *J Neuroendocrinol*. 2009;21:813–821.
40. **Wakabayashi Y, Nakada T, Murata K, et al.** Neurokinin B and dynorphin A in kisspeptin neurons of the arcuate nucleus participate in generation of periodic oscillation of neural activity driving pulsatile gonadotropin-releasing hormone secretion in the goat. *J Neurosci*. 2010;30:3124–3132.
41. **Seminara SB, Messager S, Chatzidaki EE, et al.** The GPR54 gene as a regulator of puberty. *N Engl J Med*. 2003;349:1614–1627.
42. **Navarro VM, Gottsch ML, Chavkin C, Okamura H, Clifton DK, Steiner RA.** Regulation of gonadotropin-releasing hormone secretion by kisspeptin/dynorphin/neurokinin B neurons in the arcuate nucleus of the mouse. *J Neurosci*. 2009;29:11859–11866.
43. **Mittelman-Smith MA, Williams H, et al.** Arcuate kisspeptin/neurokinin B/dynorphin (KNDy) neurons mediate the estrogen suppression of gonadotropin secretion and body weight. *Endocrinology*. 2012;153:2800–2812.
44. **Mittelman-Smith MA, Williams H, Krajewski-Hall SJ, McMullen NT, Rance NE.** Role for kisspeptin/neurokinin B/dynorphin (KNDy) neurons in cutaneous vasodilatation and the estrogen modulation of body temperature. *Proc Natl Acad Sci USA*. 2012;109:19846–19851.
45. **Cheng G, Coolen LM, Padmanabhan V, Goodman RL, Lehman MN.** The kisspeptin/neurokinin B/dynorphin (KNDy) cell population of the arcuate nucleus: sex differences and effects of prenatal testosterone in sheep. *Endocrinology*. 2010;151:301–311.
46. **Walker DM, Kirson D, Perez LF, Gore AC.** Molecular profiling of postnatal development of the hypothalamus in female and male rats. *Biol Reprod*. 2012;87:129.
47. **Eghlidi DH, Haley GE, Noriega NC, Kohama SG, Urbanski HF.** Influence of age and 17β-estradiol on kisspeptin, neurokinin B, and prodynorphin gene expression in the arcuate-median eminence of female rhesus macaques. *Endocrinology*. 2010;151:3783–3794.
48. **Cholanian M, Krajewski-Hall SJ, Levine RB, McMullen NT, Rance NE.** Electrophysiology of arcuate neurokinin B neurons in female Tac2-EGFP transgenic mice. *Endocrinology*. 2014;155:2555–2565.
49. **Yang JJ, Caligioni CS, Chan YM, Seminara SB.** Uncovering novel reproductive defects in neurokinin B receptor null mice: closing the gap between mice and men. *Endocrinology*. 2012;153:1498–1508.
50. **Rance NE, McMullen NT, Smialek JE, Price DL, Young WS 3rd.** Postmenopausal hypertrophy of neurons expressing the estrogen receptor gene in the human hypothalamus. *J Clin Endocrinol Metab*. 1990;71:79–85.
51. **Rometo AM, Krajewski SJ, Voytko ML, Rance NE.** Hypertrophy and increased kisspeptin gene expression in the hypothalamic infundibular nucleus of postmenopausal women and ovariectomized monkeys. *J Clin Endocrinol Metab*. 2007;92:2744–2750.
52. **Rometo AM, Rance NE.** Changes in prodynorphin gene expression and neuronal morphology in the hypothalamus of postmenopausal women. *J Neuroendocrinol*. 2008;20:1376–1381.
53. **Abel TW, Rance NE.** Stereologic study of the hypothalamic infundibular nucleus in young and older women. *J Comp Neurol*. 2000;424:679–688.
54. **Kermath BA, Gore AC.** Neuroendocrine control of the transition to reproductive senescence: lessons learned from the female rodent model. *Neuroendocrinology*. 2012;96:1–12.
55. **Kim W, Jessen HM, Auger AP, Terasawa E.** Postmenopausal increase in KiSS-1, GPR54, and luteinizing hormone releasing hormone (LHRH-1) mRNA in the basal hypothalamus of female rhesus monkeys. *Peptides*. 2009;30:103–110.
56. **Rance NE, Bruce TR.** Neurokinin B gene expression is increased in the arcuate nucleus of ovariectomized rats. *Neuroendocrinology*. 1994;60:337–345.
57. **Fitzgerald K, Zucker I.** Circadian organization of the estrous cycle of the golden hamster. *Proc Natl Acad Sci USA*. 1976;73:2923–2927.
58. **Kriegsfeld LJ, Silver R.** The regulation of neuroendocrine function: timing is everything. *Horm Behav*. 2006;49:557–574.
59. **Carmichael MS, Nelson RJ, Zucker I.** Hamster activity and estrous cycles: control by a single versus multiple circadian oscillator(s). *Proc Natl Acad Sci USA*. 1981;78:7830–7834.
60. **Miller BH, Takahashi JS.** Central circadian control of female reproductive function. *Front Endocrinol*. 2013;4:195.
61. **Hardin PE, Hall JC, Rosbash M.** Feedback of the *Drosophila* period gene product on circadian cycling of its messenger RNA levels. *Nature*. 1990;343:536–540.
62. **Reppert SM, Weaver DR.** Coordination of circadian timing in mammals. *Nature*. 2002;418:935–941.
63. **Roenneberg T, Merrow M.** The network of time: understanding the molecular circadian system. *Curr Biol*. 2003;13:R198–R207.
64. **Rutila JE, Suri V, Le M, So WV, Rosbash M, Hall JC.** CYCLE is a second bHLH-PAS clock protein essential for circadian rhythmicity and transcription of *Drosophila* period and timeless. *Cell*. 1998;93:805–814.
65. **Allada R, White NE, So WV, Hall JC, Rosbash M.** A mutant *Drosophila* homolog of mammalian Clock disrupts circadian rhythms and transcription of period and timeless. *Cell*. 1998;93:791–804.
66. **Dolatshad H, Campbell EA, O'Hara L, Maywood ES, Hastings MH, Johnson MH.** Developmental and reproductive performance in circadian mutant mice. *Hum Reprod*. 2006;21:68–79.
67. **Miller BH, Olson SL, Turek FW, Levine JE, Horton TH, Takahashi JS.** Circadian clock mutation disrupts estrous cyclicity and maintenance of pregnancy. *Curr Biol*. 2004;14:1367–1373.
68. **Nakamura TJ, Shinohara K, Funabashi T, Kimura F.** Effect of estrogen on the expression of Cry1 and Cry2 mRNAs in the suprachiasmatic nucleus of female rats. *Neurosci Res*. 2001;41:251–255.
69. **Shinohara K, Funabashi T, Nakamura TJ, Kimura F.** Effects of estrogen and progesterone on the expression of connexin-36 mRNA in the suprachiasmatic nucleus of female rats. *Neurosci Lett*. 2001;309:37–40.
70. **Wyse CA, Coogan AN.** Impact of aging on diurnal expression

patterns of CLOCK and BMAL1 in the mouse brain. *Brain Res*. 2010;1337:21–31.
71. **Kriegsfeld LJ, Korets R, Silver R.** Expression of the circadian clock gene Period 1 in neuroendocrine cells: an investigation using mice with a Per1::GFP transgene. *Eur J Neurosci*. 2003;17:212–220.
72. **Yamazaki S, Straume M, Tei H, Sakaki Y, Menaker M, Block GD.** Effects of aging on central and peripheral mammalian clocks. *Proc Natl Acad Sci USA*. 2002;99:10801–10806.
73. **Hastings MH, Reddy AB, Maywood ES.** A clockwork web: circadian timing in brain and periphery, in health and disease. *Nature Rev Neurosci*. 2003;4:649–661.
74. **Bailey M, Silver R.** Sex differences in circadian timing systems: implications for disease. *Front Neuroendocrinol*. 2014;35:111–139.
75. **Walker DM, Goetz BM, Gore AC.** Dynamic postnatal developmental and sex-specific neuroendocrine effects of prenatal polychlorinated biphenyls in rats. *Mol Endocrinology*. 2014;28:99–115.
76. **Lin L, Faraco J, Li R, et al.** The sleep disorder canine narcolepsy is caused by a mutation in the hypocretin (orexin) receptor 2 gene. *Cell*. 1999;98:365–376.
77. **Székely M.** Orexins, energy balance, temperature, sleep-wake cycle. *Am J Physiol Regul Integr Comp Physiol*. 2006;291:R530–R532.
78. **Adachi S, Yamada S, Takatsu Y, et al.** Involvement of anteroventral periventricular metastin/kisspeptin neurons in estrogen positive feedback action on luteinizing hormone release in female rats. *J Reprod Dev*. 2007;53:367–378.
79. **Irwig MS, Fraley GS, Smith JT, et al.** Kisspeptin activation of gonadotropin releasing hormone neurons and regulation of KiSS-1 mRNA in the male rat. *Neuroendocrinology*. 2004;80:264–272.
80. **Messager S, Chatzidaki EE, Ma D, et al.** Kisspeptin directly stimulates gonadotropin-releasing hormone release via G protein-coupled receptor 54. *Proc Natl Acad Sci USA*. 2005;102:1761–1766.
81. **Parhar IS, Ogawa S, Sakuma Y.** Laser-captured single digoxigenin-labeled neurons of gonadotropin-releasing hormone types reveal a novel G protein-coupled receptor (Gpr54) during maturation in cichlid fish. *Endocrinology*. 2004;145:3613–3618.
82. **Uenoyama Y, Inoue N, Pheng V, et al.** Ultrastructural evidence of kisspeptin-gonadotrophin-releasing hormone (GnRH) interaction in the median eminence of female rats: implication of axo-axonal regulation of GnRH release. *J Neuroendocrinol*. 2011;23:863–870.
83. **Lederman MA, Lebesgue D, Gonzalez VV, et al.** Age-related LH surge dysfunction correlates with reduced responsiveness of hypothalamic anteroventral periventricular nucleus kisspeptin neurons to estradiol positive feedback in middle-aged rats. *Neuropharmacology*. 2010;58:314–320.
84. **Zheng W, Jimenez-Linan M, Rubin BS, Halvorson LM.** Anterior pituitary gene expression with reproductive aging in the female rat. *Biol Reprod*. 2007;76:1091–1102.
85. **Naugle MM, Nguyen LT, Merceron TK, et al.** G-protein coupled estrogen receptor, estrogen receptor α, and progesterone receptor immunohistochemistry in the hypothalamus of aging female rhesus macaques given long-term estradiol treatment. *J Exp Zool Part A Ecol Genet Physiol*. 2014;321:399–414.
86. **Herbison AE, Horvath TL, Naftolin F, Leranth C.** Distribution of estrogen receptor-immunoreactive cells in monkey hypothalamus: relationship to neurones containing luteinizing hormone-releasing hormone and tyrosine hydroxylase. *Neuroendocrinology*. 1995;61:1–10.
87. **Pelletier G, Labrie C, Labrie F.** Localization of oestrogen receptor α, oestrogen receptor β and androgen receptors in the rat reproductive organs. *J Endocrinol*. 2000;165:359–370.
88. **Schechter J, Weiner R.** Changes in basic fibroblast growth factor coincident with estradiol-induced hyperplasia of the anterior pituitaries of Fischer 344 and Sprague-Dawley rats. *Endocrinology*. 1991;129:2400–2408.
89. **Robl JM, Thomford PJ, Wu MC, Dziuk PJ.** Effect of estrogen, testosterone, and phenobarbital on uterine weight and liver microsomal enzymes in prepuberal mice. *Pediatr Pharmacol*. 1985;5:157–164.
90. **Kawakami M, Yoshioka E, Konda N, Arita J, Visessuvan S.** Data on the sites of stimulatory feedback action of gonadal steroids indispensable for luteinizing hormone release in the rat. *Endocrinology*. 1978;102:791–798.
91. **Keefer DA, Stumpf WE, Petrusz P.** Quantitative autoradiographic assessment of 3H-estradiol uptake in immunocytochemically characterized pituitary cells. *Cell Tissue Res*. 1976;166:25–35.
92. **D'Angelo SA, Fisher JS.** Influence of estrogen on the pituitary-thyroid system of the female rat: mechanisms and loci of action. *Endocrinology*. 1969;84:117–122.
93. **Chen HJ, Walfish PG.** Effects of estradiol benzoate on thyroid-pituitary function in female rats. *Endocrinology*. 1978;103:1023–1030.
94. **Fisher JS, D'Angelo SA.** Stimulatory and inhibitory action of estradiol on TSH secretion. *Endocrinology*. 1971;88:687–691.
95. **Schindler AE.** Thyroid function and postmenopause. *Gynecol Endocrinol*. 2003;17:79–85.
96. **Pearce EN.** Thyroid dysfunction in perimenopausal and postmenopausal women. *Menopause Intl*. 2007;13:8–13.
97. **Farbota L, Hofmann C, Oslapas R, Paloyan E.** Sex hormone modulation of serum TSH levels. *Surgery*. 1987;102:1081–1087.
98. **Böttner M, Wuttke W.** Chronic treatment with low doses of estradiol affects pituitary and thyroid function in young and middle-aged ovariectomized rats. *Biogerontology*. 2005;6:261–269.
99. **Viau V, Meaney MJ.** Variations in the hypothalamic-pituitary-adrenal response to stress during the estrous cycle in the rat. *Endocrinology*. 1991;129:2503–2511.
100. **Burgess LH, Handa RJ.** Chronic estrogen-induced alterations in adrenocorticotropin and corticosterone secretion, and glucocorticoid receptor-mediated functions in female rats. *Endocrinology*. 1992;131:1261–1269.
101. **Carey MP, Deterd CH, de Koning J, Helmerhorst F, de Kloet ER.** The influence of ovarian steroids on hypothalamic-pituitary-adrenal regulation in the female rat. *J Endocrinol*. 1995;144:311–321.
102. **Li J, Daly E, Campioli E, Wabitsch M, Papadopoulos V.** De novo synthesis of steroids and oxysterols in adipocytes. *J Biol Chem*. 2014;289:747–764.
103. **Sanathara NM, Moreas J, Mahavongtrakul M, Sinchak K.** Estradiol upregulates progesterone receptor and orphanin FQ colocalization in arcuate nucleus neurons and opioid receptor-like receptor-1 expression in proopiomelanocortin neurons that project to the medial preoptic nucleus in the female rat. *Neuroendocrinology*. 2014;103–118.
104. **Sprangers SA, Fahrenbach WH, Bethea CL.** Steroid action on estrogen and progestin receptors in monkey pituitary cell cultures. *Endocrinology*. 1991;128:1907–1917.
105. **Heinzlmann A, Köves K.** The characteristic change in the distribution of S-100 immunoreactive folliculostellate cells in rat anterior pituitary upon long-term estrogen treatment is prevented by concomitant progesterone treatment. *Endocrine*. 2008;33:342–348.
106. **Huang SK, Pan JT.** Stimulatory effects of vasoactive intestinal peptide and pituitary adenylate cyclase-activating peptide on tuberoinfundibular dopaminergic neuron activity in estrogen-treated ovariectomized rats and their correlation with prolactin secretion. *Neuroendocrinology*. 1996;64:208–214.
107. **Xu B, Goulding EH, Zang K, et al.** Brain-derived neurotrophic factor regulates energy balance downstream of melanocortin-4 receptor. *Nature Neurosci*. 2003;6:736–742.
108. **Scharfman HE, MacLusky NJ.** Estrogen and brain-derived neurotrophic factor (BDNF) in hippocampus: complexity of steroid

hormone-growth factor interactions in the adult CNS. *Front Neuroendocrinol*. 2006;27:415–435.
109. **Höpker VH, Amoureux MC, Varon S.** NGF and BDNF in the anterior pituitary lobe of adult rats. *J Neurosci Res*. 1997;49:355–363.
110. **Nakahashi T, Fujimura H, Altar CA, et al.** Vascular endothelial cells synthesize and secrete brain-derived neurotrophic factor. *FEBS Lett*. 2000;470:113–117.
111. **Fujimura H, Altar CA, Chen R, et al.** Brain-derived neurotrophic factor is stored in human platelets and released by agonist stimulation. *Thromb Haemostasis*. 2002;87:728–734.
112. **Poehlman ET, Toth MJ, Gardner AW.** Changes in energy balance and body composition at menopause: a controlled longitudinal study. *Ann Int Med*. 1995;123:673–675.
113. **Toth MJ, Tchernof A, Sites CK, Poehlman ET.** Menopause-related changes in body fat distribution. *Ann NY Acad Sci*. 2000;904:502–506.
114. **Carr MC.** The emergence of the metabolic syndrome with menopause. *J Clin Endocrinol Metab*. 2003;88:2404–2411.
115. **Tarttelin MF, Gorski RA.** The effects of ovarian steroids on food and water intake and body weight in the female rat. *Acta Endocrinol (Copenh)*. 1973;72:551–568.
116. **Heine PA, Taylor JA, Iwamoto GA, Lubahn DB, Cooke PS.** Increased adipose tissue in male and female estrogen receptor-α knockout mice. *Proc Natl Acad Sci USA*. 2000;97:12729–12734.
117. **Jones ME, Thorburn AW, Britt KL, et al.** Aromatase-deficient (ArKO) mice have a phenotype of increased adiposity. *Proc Natl Acad Sci USA*. 2000;97:12735–12740.
118. **Mook DG, Kenney NJ, Roberts S, Nussbaum AI, Rodier WI 3rd.** Ovarian-adrenal interactions in regulation of body weight by female rats. *J Comp Physiol Psychiatr*. 1972;81:198–211.
119. **Landau IT, Zucker I.** Estrogenic regulation of body weight in the female rat. *Horm Behav*. 1976;7:29–39.
120. **Gao Q, Mezei G, Nie Y, et al.** Anorectic estrogen mimics leptin's effect on the rewiring of melanocortin cells and Stat3 signaling in obese animals. *Nature Med*. 2007;13:89–94.
121. **Clegg DJ, Riedy CA, Smith KA, Benoit SC, Woods SC.** Differential sensitivity to central leptin and insulin in male and female rats. *Diabetes*. 2003;52:682–687.
122. **Rogers NH, Perfield JW 2nd, Strissel KJ, Obin MS, Greenberg AS.** Reduced energy expenditure and increased inflammation are early events in the development of ovariectomy-induced obesity. *Endocrinology*. 2009;150:2161–2168.
123. **Adams MM, Fink SE, Shah RA, et al.** Estrogen and aging affect the subcellular distribution of estrogen receptor-α in the hippocampus of female rats. *J Neurosci*. 2002;22:3608–3614.
124. **Maffucci JA, Gore AC.** Age-related changes in hormones and their receptors in animal models of female reproductive senescence. In: Conn MP, ed. *Handbook of Models for Human Aging*. San Diego, CA: Academic Press, 2006:533–552.
125. **Walker ML, Herndon JG.** Menopause in nonhuman primates? *Biol Reprod*. 2008;79:398–406.
126. **Hoyer PB, Sipes IG.** Assessment of follicle destruction in chemical-induced ovarian toxicity. *Ann Rev Pharmacol Toxicol*. 1996;36:307–331.
127. **Springer LN, McAsey ME, Flaws JA, Tilly JL, Sipes IG, Hoyer PB.** Involvement of apoptosis in 4-vinylcyclohexene diepoxide-induced ovotoxicity in rats. *Toxicol Appl Pharmacol*. 1996;139:394–401.
128. **Acosta JI, Mayer L, Talboom JS, et al.** Transitional versus surgical menopause in a rodent model: etiology of ovarian hormone loss impacts memory and the acetylcholine system. *Endocrinology*. 2009;150:4248–4259.
129. **Van Kempen TA, Milner TA, Waters EM.** Accelerated ovarian failure: a novel, chemically induced animal model of menopause. *Brain Res*. 2011;1379:176–187.